Biomedicine & Pharmacotherapy 110 (2019) 482–492

Contents lists available at ScienceDirect

Biomedicine & Pharmacotherapy

journal homepage: www.elsevier.com/locate/biopha

Neuroprotection and improvement of the histopathological and behavioral impairments in a murine Alzheimer's model treated with *Zephyranthes carinata* alkaloids

Natalie Cortes[a], Angelica Maria Sabogal-Guaqueta[b], Gloria Patricia Cardona-Gomez[b], Edison Osorio[a,*]

[a] Grupo de Investigación en Sustancias Bioactivas, Facultad de Ciencias Farmacéuticas y Alimentarias, Universidad de Antioquía UdeA, Calle 70 No, 52-21, Medellin, Colombia

[b] Neuroscience Group of Antioquia, Cellular and Molecular Neurobiology Area - School of Medicine, SIU, University of Antioquia UdeA, Calle 70 No, 52-21, Medellin, Colombia

ARTICLE INFO

Keywords:
Alzheimer's disease
Zephyranthes carinata
Amaryllidaceae alkaloids
Tau
Behavior function
Inflammation

ABSTRACT

In Alzheimer's disease (AD), amyloid beta (Aβ) plaques initiates a cascade of pathological events where the overactivation of *N*-methyl-D-aspartate receptors (NMDA) by excess glutamate (Glu) triggers oxidative processes that lead to the activation of microglial cells, inflammation, and finally neuronal death. Amaryllidaceae alkaloids exert neuroprotective activities against different neurotoxin-induced injuries *in vitro*, and although their biological potential is well demonstrated, their neuroprotective activity has not been reported in an *in vivo* model of AD. The aim of our study was to determine the *in vitro* and *in vivo* neuroprotective potential of standardized alkaloidal fractions of *Zephyranthes carinata*. In this work, the neuroprotective effect of two alkaloidal fractions extracted from *Z. carinata* (bulbs and leaves) was analyzed in an *in vitro* excitotoxicity model in order to select the most promising one for subsequent evaluation in a triple transgenic mouse model of AD (3xTg-AD). We found that *Z. carinata* bulbs protect neurons against a Glu-mediated toxic stimulus *in vitro*, as evidenced by the decrease in apoptotic nuclei, the reduction in the lipid peroxidation product malondialdehyde and the conservation of dendritic structures. The effects of intraperitoneal administration of *Z. carinata* bulbs (10 mg/kg) every 12 h for 1 month on 3xTg-AD (18 months old) showed improved learning and spatial memory. Histopathologically, the alkaloidal fraction-treated 3xTg-AD mice exhibited a significant reduction in tauopathy and astrogliosis, as well as a significant decrease in the proinflammatory marker COX-2 and an increase in pAkt. The results suggest that *Z. carinata* bulbs provide neuroprotective effects both *in vitro* and in 3xTg-AD mice by intervening in the inflammatory processes, regulating the aggregation of pair helical filaments (PHFs) and activating survival pathways.

1. Introduction

Alzheimer's disease (AD) is the main cause of dementia and affects more than 50 million people in the world [1,2]. At the clinical level, AD is characterized by a decrease in episodic memory that, over time, leads to a stronger decline in general cognitive abilities, mainly the loss of

Abbreviations: 3xTg-AD, homozygous triple transgenic mouse model; Ach, acetylcholine; AChE, acetylcholinesterase; AD, Alzheimer's disease; AKT, serine-threonine protein kinase; AMDIS, automated mass spectral deconvolution and identification system; ANOVA, analysis of variance; Aβ, amyloid beta; B, bulbs; BSA, bovine serum albumin; BChE, butyrylcholinesterase; CA1, first region in the hippocampal circuit; CDK5, cyclin-dependent kinase 5; COX-2, cyclooxygenase 2; DAB, diaminobenzidine; DIV, day *in vitro*; DMSO, dimethyl sulfoxide; E18, wistar rat embryos; EC, entorhinal cortex; FDA, Food and Drug Administration; GC/MS, gas chromatography/mass spectrometry; GFAP, glial fibrillary acidic protein; Glu, glutamate; Iba1, ionized calcium binding adaptor molecule; iNOS, inducible nitric oxide synthase; LDH, lactate dehydrogenase; MAP2, anti-microtubule associated protein 2 antibody; MAPK, mitogen-activated protein kinases; MDA, malondialdehyde; MWM, Morris water maze; NADH, nicotinamide adenine dinucleotide NFTs intracellular neurofibrillary tangles; NIST, mass spectral database; NMDA, *N*-methyl-D-aspartate receptors; PBS, phosphate-buffered saline; PHFs, paired helical filaments; PLA2, phospholipase A2; RI, Kovats retention indexes; SDS, sodium dodecyl sulfate; TBA, thiobarbituric acid; TBARS, thiobarbituric acid reactive substances; TEP, 11,3,3-tetraethoxypropane

* Corresponding author.
E-mail address: edison.osorio@udea.edu.co (E. Osorio).

https://doi.org/10.1016/j.biopha.2018.12.013
Received 12 September 2018; Received in revised form 10 November 2018; Accepted 2 December 2018

long-term memories, changes in personality and the loss of language and attention [3]. Histopathologically, AD is characterized by the formation of two protein aggregates: extracellular amyloid-beta (Aβ) and phosphorylated tau developing into intracellular neurofibrillary tangles (NFTs), which are responsible for the degeneration of hippocampal, cortical, and subcortical neurons [4]. Several studies have shown that Aβ oligomers have a leading role in the mechanisms of synaptic deterioration and neuronal damage in AD [5], since the deposition of Aβ in different areas of the brain, especially those involved in cognitive processes, triggers excitotoxic stimuli mediated by the neurotransmitter glutamate (Glu). As a result, there is an increase in the intraneuronal concentration of Ca^{2+}, causing stress-related signaling pathways and free radical generation, which exacerbate synaptic dysfunction and promote the increase of oxidative stress, inflammatory processes, lipid peroxidation, tau phosphorylation and eventually neuronal death [6,7].

Due to the complexity of AD, the pharmacological intervention from both the palliative and prophylactic and/or modulatory approaches to the disease provides a potential field for the development of new drugs. Although, to date, the number of drugs approved by the Food and Drug Administration (FDA) for AD is limited [8], cholinergic and glutamatergic therapy led by acetylcholinesterase (AChE) enzyme inhibitors and *N*-methyl-D-aspartate receptor (NMDA) blockers, respectively, have been at the forefront of efforts to improve the symptoms and quality of life of patients with AD. In fact, other types of therapeutic alternatives have been proposed where the reductionist paradigm 'one-drug-one-target', which has dominated the discovery of drugs in recent decades, has been challenged, and a more holistic approach has recently emerged [9]. The symbiosis of the approved drugs (inhibitors of AChE + blockers of NMDA) has shown significant cognitive enhancement in animal models after their administration, since the combination treatment blocks the toxic effects associated with excess glutamate and prevents the hydrolysis of acetylcholine (ACh) in the brain [10,11]. Although, the polypharmacological strategy remains a matter of dispute, this approach that simultaneously modulates multiple targets is increasingly perceived as an attractive opportunity to intervene in the progress of AD.

Previous works have focused on natural compounds and their derivatives as potential multi-pharmacological anti-AD agents [12]. However, galantamine, an alkaloid with inhibitory activity on AChE, is the only FDA-approved drug that is naturally occurring and that is extracted from plants of the Amaryllidaceae family, one of the 20 most important alkaloid-containing plant families [13]. In fact, the Amaryllidaceae species are a source of unique alkaloids (Amaryllidaceae alkaloids) that exhibit remarkable inhibition of AChE activity [13], but they are also able to protect neurons against different toxic stimuli *in vitro* [13–15]. Different extracts that are rich in Amaryllidaceae alkaloids have simultaneously presented AChE inhibitory activity and neuroprotective activity in an *in vitro* model of Glu excitotoxicity [16,17], such as *Zephyranthes carinata* Herb., one of the plant species that has stood out for its biological activity. Although there are few reports of the *in vivo* activity of the Amaryllidaceae [18,19], the emergent polypharmacological evidence for the treatment of AD has placed the Amaryllidaceae alkaloids in the spotlight, and their *in vitro* potential is an important starting point as a platform for the evaluation of *in vivo* models for AD. Therefore, we evaluated the *in vitro* neuroprotective potential of two standardized alkaloidal fractions of *Z. carinata* (bulbs and leaves, namely *Z. carinata* B and *Z. carinata* L) through a model of Glu excitotoxicity. The most promising fraction was evaluated in an *in vivo* model of triple transgenic mice for AD. In this study, it is tried to know if the *in vitro* anteroom is robust enough to postulate a fraction as a possible neuroprotective agent in an *in vivo* model for AD, which presents the histopathological and cognitive characteristics of the disease.

2. Materials and methods

2.1. Plant material and alkaloid extraction

The plant material (*Z. carinata*) was collected in the Department of Antioquia during the flowering period between February and April 2014. A representative specimen of the species (4263 Alzate) was kept at the herbarium of the University of Antioquia (Medellín, Colombia). The collected plant material was dried in an oven at 40 °C for several days and powdered before extraction. Extraction of the alkaloidal fraction was performed under the same parameters as the previous reports [20].

2.2. GC/MS analysis

The capillary gas chromatography/mass spectrometry (GC/MS) analyses were recorded on a GC/MS 7890, operating in EI mode at 70 eV A HP-1 MS capillary column (30 m x 0.25 mm x 0.25 um) was used. The temperature program was: 1 min hold at 120 °C, 120–210 °C at 15 °C min^{-1}, 210–260 at 8 °C min^{-1} and 260–300 °C at 15 °C min^{-1}. Injector temperature was 280 °C in splitless mode. The flow rate of carrier gas (helium) was 1 mL min^{-1}. One microliter of the solution was injected. The alkaloids were identified comparing the mass spectral fragmentation of the compounds with standard reference spectra from NIST database (NIST Mass Spectral Database, (2008), National Institute of Standardization and Technology, USA), and comparing the obtained spectra with those reported in the literature. An alternative identification of the alkaloids was performed by comparing their GC/MS spectra with private library database. This library has been regularly updated with alkaloids isolated and unequivocally identified *via* physical and spectroscopic means [21]. Mass spectra were deconvoluted using AMDIS 2.64 software (NIST). Kovats retention indexes (RI) of the compounds were recorded with standard calibration n-hydrocarbon mixture (C_7 - C_{40}) using AMDIS 2.64 software. The proportion of each individual compound in the alkaloid fractions was expressed as percentage of the total alkaloids (Table 1). The area of the GC/MS peaks depends not only on the concentration of the corresponding compounds but also on the intensity of their mass spectral fragmentation. Therefore, data given in Table 1 do not express a real quantification, although they can be used to compare the samples [22].

2.3. In vitro studies

2.3.1. Primary neuronal cultures

Cerebral cortices from Wistar rat embryos (E18) were dissected, trypsinized and dissociated [23]. The dissociated cells were then cultured on poly-L-lysine (Sigma-Aldrich) precoated multi-well plates in neurobasal medium (GIBCO) containing a B-27 supplement (Sigma-Aldrich) and a penicillin–streptomycin antibiotic mixture (GIBCO) at 37 °C under a 5% CO_2 humidified atmosphere. Neurons that were isolated and dissociated as described above were plated at a density of 500 cells/mm^2 (equivalent to 100,000 per well) in 24-well plates for immunofluorescence and cytotoxicity assays at a density of 250 cell/mm^2 (50,000 per well) in 96-well plates. Neurons for the cytotoxicity assays were plated at a density of 50,000 cells/well, alkaloidal fractions were dissolved in DMSO and the solutions were then diluted in culture media at six concentrations (0.75 μg/mL, 1.5 μg/mL, 3.0 μg/mL, 6.0 μg/mL, 12.0 μg/mL, and 24.0 μg/mL). The solutions were added to the culture at DIV 6, and the plates were incubated at 37 °C with 5% CO_2 for 48 h. Then, 120 μL of supernatant was mixed with the LDH kit (Roche), and the absorbance was measured at 490 nm using a BioTek Synergy 2 reader (BioTek, USA). All samples were cultured three times in duplicate each time.

2.3.2. LDH release

A cytotoxicity detection kit (Roche) was used to assess the presence

Table 1
Composition of the alkaloidal fractions of *Zephyranthes carinata* Herb.

					Z. carinata B		*Z. carinata* L	
Item[a]	Name	M+	Ions	RI	ng/mg[d]	% relative[e]	ng/mg	% relative
1	Trisphaeridine	223 (100)[b]	164 (15), 138 (25), 111 (19)	2197[c]	0,0080	14,20	0,0079	17,24
2	M+ 239	238 (100)	180 (11), 118 (9), 90 (10)	2235	0,0004	0,77	0,0000	0,00
3	Galanthamine	287 (78)	270 (14), 244 (24), 216 (36), 174 (35), 115 (18)	2295	0,0016	2,87	0,0021	4,67
4	Lycoramine	289 (57)	288 (100)	2313	0,0161	28,71	0,0135	29,25
5	Vittatine	271 (100)	252 (26), 228 (24), 199 (79), 187 (71), 129 (25), 115 (35)	2357	0,0059	10,48	0,0093	20,16
6	11,12-dehydroanhydrolycorine	249 (57)	248 (100), 190 (25), 95 (20)	2473	0,0029	5,24	0,0034	7,43
7	M+ 329	329 (74)	257 (100), 225 (31), 199 (28), 139 (11), 115 (12)	2535	0,0011	1,96		
8	Tazettine	331 (23)	316 (12), 298 (18), 247 (100), 227 (12), 201 (18), 181 (16), 115 (16), 70 (31)	2543	0,0034	5,99		
9	M+ 343	343 (5)	269 (100), 240 (39), 224 (28), 211 (20), 181 (72), 153 (18), 115 (24)	2549	0,0000	0,02	0,0029	6,30
10	Galantine	317 (19)	298 (8), 268 (14), 243 (90), 242 (100), 162 (10), 125 (11)	2597	0,0126	22,43	0,0024	5,18
11	Lycorine	287 (22)	268 (19), 250 (22), 227 (62), 226 (100)	2603	0,0008	1,49		
12	Undulatine isomer	331(100)	286 (16), 258 (33), 217 (30), 205 (65), 189 (40), 173 (33), 145 (13), 115 (25)	2606			0,0015	3,27
13	M+ 295	295 (85)	294 (100), 278 (12), 147 (11)	2814	0,0033	5,83	0,0030	6,51

[a] Peak numbering of signals in the chromatogram.
[b] Percentage of the signal in the mass spectrum.
[c] Relative retention index (Kovats retention index) of compounds in HP1 capillary column.
[d] ng alkaloid per mg of alkaloidal fraction.
[e] Percentage of the alkaloid regarding content of total alkaloids detected.

of cytotoxicity by measuring the activity of lactate dehydrogenase (LDH) released by cultures. The culture medium was recovered two days after the treatments with alkaloidal fractions (DIV 8). LDH activity was determined by measuring NADH absorption as the linear rate of consumption during pyruvate reduction to lactate using a BioTek Synergy 2 reader. The cytotoxicity was calculated for a given test condition using the following equation: cytotoxicity (%) = [(A − low control) / (high control − low control)] × 100, where A is the mean LDH activity measured in the media samples from three wells per duplicate that were subjected to the test condition, low control is the LDH activity released from untreated normal cells, and high control is the maximum LDH activity released in all cells (cells treated with 1% Triton X-100 for 24 h).

2.3.3. Neuroprotection assay

The neuron cultures were pre- and posttreated with alkaloidal fractions. DIV 6 neurons were first pretreated with alkaloidal fractions at concentrations of 0.75 µg/mL, 1.5 µg/mL, 3.0 µg/mL and 6.0 µg/mL, and DIV 7 neurons were treated with 125 µM glutamate (toxic stimulus; Sigma-Aldrich) and 1X glutamate buffer (pH = 7) for 20 min [24]. The posttreated DIV 7 neurons were first treated with glutamate 125 µM and 1X glutamate buffer for 20 min and then posttreated with alkaloids at the same concentrations as the pretreated neurons. In both treatments, the media were collected at DIV 8 and then LDH was quantified.

2.3.4. Immunofluorescence

Cultures were fixed in 4% formaldehyde prepared in a cytoskeleton buffer for 20 min [25]. Autofluorescence was blocked with 50 mM NH_4Cl. Cells were permeabilized and blocked with PBS + 0.1% Triton X-100 and 1% fetal bovine serum for 1 h. Cultures were incubated overnight at 4 °C with the following primary antibodies: MAP2 (1:2000) (Sigma-Aldrich), Alexa 488 (1:2000) and Alexa 594 (1:1000) (Molecular Probes). Secondary fluorescent antibodies were used as probes. Nuclei were stained with Hoechst 33,258 (1:5000) (Invitrogen) for 1 h. Neurons were washed four times in buffer, cover slipped using Gel Mount (Biomeda) and observed with an Olympus IX epifluorescence microscope (Olympus) or DSU Spinning Disc confocal microscope (Olympus). No staining was observed when primary antibodies were omitted. Image processing X–Y images were collected using an Olympus IX 81 epifluorescence microscope with a 40x (NA, 1.3) or 60x (NA, 1.42) oil immersion objective.

2.3.5. Quantitative image analysis

The percentage of condensed nuclei was obtained using the following formula: [condensed nuclei / (condensed nuclei + normal nuclei)] × 100 [26]. The mean area, diameter and intensity of each nucleus were quantified using the automatic measurement/spatial trace feature tool. Condensed nuclei were defined as those possessing an average area equal to or less than 40 μm^2, a diameter equal to or less than 6 µm and a fluorescence intensity equal to or greater than 120 (AU). Condensed nuclei were quantified in five 40x fields. For each intensity measurement, the background field was subtracted, and comparisons were performed from parallel experiments [27]. Images were analyzed individually and calibrated to a micrometer scale using Image Scope Pro Plus software (Media Cybernetics). Analyses were performed for 30 neurons per treatment in each duplicate assay and for at least four independent experiments (n = 4).

2.3.6. Thiobarbituric acid reactive substances (TBARS) assay

This assay was carried out using the colorimetric technique described previously [28] with some modifications. Neurons and supernatant remnants were suspended and lysate with SDS (Sigma-Aldrich) (1% final concentration). Then, 250 µL of a solution of 0.67% thiobarbituric acid (TBA) (Sigma-Aldrich), 15% trichloroacetic acid (Merck) and 0.1 M HCl (Merck) was added to 250 µL of cell lysate and heated to 85 °C for 30 min. After cooling in ice, the extent of lipid peroxidation was determined by TBARS method and the values were expressed as ρmol of Malondialdehyde (MDA), using 1,1,3,3-tetraethoxypropane (TEP) (Sigma-Aldrich) as standard. The absorbance to 532 nm was interpolated on the MDA calibration curve in a concentration range from 0.3125 to 20 µM.

2.4. In vivo studies

2.4.1. Animals

Homozygous triple-transgenic model (3xTg-AD) mice harboring $PS1_{M146V}$, APP_{Swe}, and Tau_{P301L} transgenes and $PS1_{M146V}$ knockin mice [29] from the in-house colony at the University of Antioquia maintained in the SIU (Sede de Investigación Universitaria) specific pathogen-free vivarium in Medellín, Colombia were used at 18 months of age to obtain a homogenous penetrance of tauopathy. The mice were maintained on a 12:12 h dark:light cycle and received food and water *ad libitum*. The animals were handled according to Colombian standards

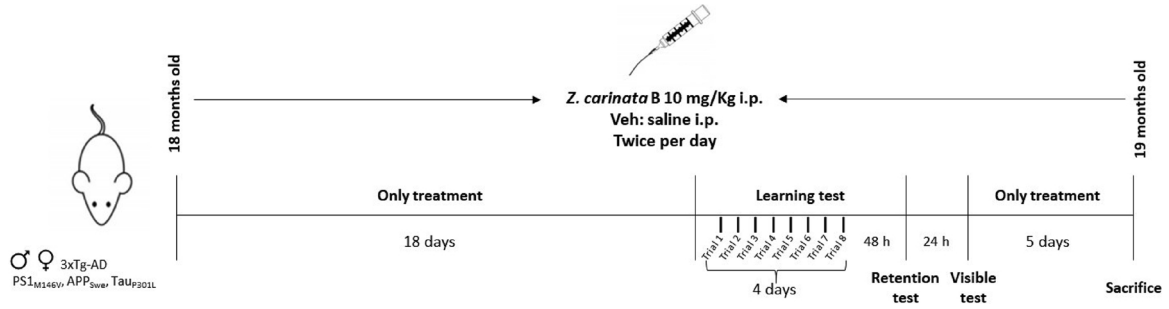

Fig. 1. Scheme of the experimental design. *Z. carinata* (10 mg/kg) or saline (Veh) were administered i.p. at 18 months old to $PS1_{M146V}$ and 3xTg-AD mice for 1 month every 12 h. Eighteen days after the first dose, learning and memory tasks were evaluated by Morris water maze test. Later, on the 30th, the mice were sacrificed for histological and biochemical analyses.

(law 84/1989 and resolution 8430/1993) and guidelines. Special care was taken to minimize animal suffering and to reduce the number of animals used.

2.4.2. Administration of alkaloidal fraction

The *Zephyranthes carinata* bulbs (Z. carinata B) fraction was dissolved in phosphate-buffered saline (PBS). The 3xTg-AD mice received 10 mg/kg of the alkaloidal fraction or saline solution (vehicle) i.p. every 12 h for 1 month beginning at 18 months of age and were sacrificed at 19 months old (Fig. 1). The alkaloidal fraction dose (10 mg/kg twice per day) and the posology of the fraction were selected based on previous studies with galantamine [30,31]. The general health conditions of the mice were carefully monitored throughout the alkaloidal fraction treatment, and no adverse effects were observed.

2.4.3. Morris water maze test

Eighteen days following first treatment, the animals were evaluated *via* the Morris water maze (MWM) test [32]. A white plastic tank 1 m in diameter and 30 cm in height was filled with water (22 ± 2 °C) to a depth of 20 cm. The platform (7 cm diameter) was 1.5 cm below the surface of the water during spatial learning and 1.5 cm above the surface of the water during the visible session. Extra-maze visual cues around the room remained in a fixed position throughout the experiment. Eight sessions or trials were performed, two complete sessions per day over four days. Each session consisted of four successive subtrials (30 s inter-trial interval), and each subtrial began with the mouse placed pseudo-randomly in one of four starting locations. The animals had been trained to stay on the platform for 30 s prior to the initial trial. If a mouse did not locate the platform after a maximum of 60 s, it was gently guided to the platform. Then, the animals were then provided with 48 h of retention time, followed by a probe trial of spatial reference memory, in which the animals were placed in the tank without the platform for 60 s (Fig. 1). To control any difference between experimental groups in the visual-motor abilities or motivation, latencies to reach the platform were evaluated with a visible platform at the end of the transfer (four trials for 1 day). Behavior was recorded by an automated system (Viewpoint, Lyon, France). Finally, some animals were perfused and others decapitated for histological and biochemical evaluation, respectively.

2.4.4. Histology

Twenty-four hours after the final dose, the animals were anesthetized intraperitoneally using a mixture of ketamine (50 mg/kg) plus xylazine (20 mg/kg) and were perfused with normal saline and 4% paraformaldehyde (0.1 M PBS, pH 7.4). Brains were removed and post-fixed with 4% paraformaldehyde at 4 °C for 48 h and then cryopreserved with 30% sucrose and stored at −20 °C. The brains were sectioned (50 μm) with a Leica VT1000S vibrating blade microtome (Leica Microsystems, Germany).

2.4.5. Immunohistochemistry

The coronal sections (50 μm) were permeabilized and blocked with 0.3% Triton X-100 and 1% BSA in PBS and were then probed with primary antibodies: anti-beta amyloid antibody (beta amyloid 1e16 (6E10) Monoclonal #SIG-39320, Covance, 1:500), anti-phospho-PHF-tau (pSer202/Thr205 Antibody (AT-8) #MN1020, Thermo Scientific, 1:500), anti-GFAP (Monoclonal Anti-Glial Fibrillary Acidic Protein, #G 3893, Sigma, 1:500), anti-Iba1 (Rabbit Anti-Iba1 (Ionized calcium binding adaptor molecule) #019-19741, Wako, 1:500) and the appropriate secondary antibodies (1:250 concentration, goat anti-rabbit IgG (H + L) biotin conjugated, Pierce #31822 or goat Anti-Mouse IgG (H + L) Biotin Conjugated Pierce #31800). Later, tissues were incubated with avidin biotin complex (ABC Standard Peroxidase Staining Kit, Pierce #32020, 1:250 reagent A:B) for 1 h. Once the complex was removed, diaminobenzidine (DAB) was used as developer. The sections were dehydrated with alcohol, cleared with xylene and sealed with Consul-mount. The immunoreactivity in the tested areas was quantified at 10x or 40x magnification and analyzed using ImageJ 1.45 software (NIH, USA). The absence of primary antibody did not result in immunoreactivity. The CA1 and subiculum (hippocampus), entorhinal cortex (EC) and amygdala were evaluated at bregma 1.76 mm posterior to bregma [33].

2.4.6. Western blotting

After the animals were sacrificed by decapitation, the hippocampus and amygdala were dissected and immediately frozen in liquid nitrogen and stored at −80 °C until analysis. The tissues were dissected and homogenized in lysis buffer according to a described previously protocol [34]. Membranes were incubated overnight with the following primary antibodies: anti-phospho-PHF-tau (pSer202/Thr205 Antibody (AT-8) #MN1020, Thermo Scientific, 1:500); anti-NOS2 (C-11) Ms mAb (# Sc 7271, Santa Cruz Biotechnology, 1:100); rabbit polyclonal anti-COX-2 (#AB15191, Abcam, 1:1000); rabbit phospho-p38 MAPK Thr180/Tyr182 (# 9215, Cell Signaling, 1:1000); phospho-AKT ser 473 (#9271, Cell Signaling Technology, Rb 1:1000), CDK5 (#SC-173, Santa Cruz, Rb 1:1000), phospho-cPLA2 Ser 505 (# 2831, Cell Signaling Technology, Rb, 1:1000), PLA2 (# 2832, Cell Signaling Technology, Rb, 1:1000) and tubulin (Mouse monoclonal anti-βIII tubulin antibody, #G712 A, Promega, 1:10000) as a loading control. IRDye 800CW goat anti-mouse or rabbit (LI-COR; diluted 1:10000) was used as a secondary probe. The blots were visualized using an Odyssey Infrared Imaging System (LI-COR Biosciences).

2.5. Statistics

At least 3 mice were used for each histological study. 4–6 mice were used for each biochemical study and 8–10 mice were used for MWM. Parametric data were evaluated with analysis of variance (ANOVA) to compare the 4 groups and then with Tukey's test for post hoc multiple comparison between-group analyses. Nonparametric data were

evaluated using the Kruskal-Wallis test. The escape latency during the training and the retention test was tested using two-way ANOVA followed by a Dunnett's post hoc test for multiple comparisons. The statistical analysis was performed using GraphPad Prism software (version 6.0), and the results were considered significant when $p < 0.05$. The values are expressed as the means ± SEM.

3. Results

3.1. Chemical characterization by GC/MS of the alkaloidal fractions of Z. carinata

To date, a large number of alkaloids extracted from plants of the Amaryllidaceae family have been effectively separated and identified by GC/MS, indicating that this method is useful and reliable for studies of the metabolism of alkaloids in this family [35]. The comparison of their fragmentation patterns and retention indices with commercial and private databases provides information on the identity and percentage contribution in the sample of the alkaloids that compose them. However, in previous works, the qualitative and quantitative differences in chemistry of each part of the Amaryllidaceae species affects its bioactivity [20]. Therefore, for this study, the leaves and bulbs were separated (*Z. carinata* L and *Z. carinata* B) for the purpose of determining the chemical and biological diversity of the plant separately. In this work, a traditional extraction of fractions rich in alkaloids was carried out. After being characterized by GC/MS, a total of 13 alkaloids of the nuclei type narciclasine, haemanthamine, lycorine, galantamine and tazettine were identified (Table 1).

3.2. Alkaloidal fraction cytotoxicity in primary cultures of rat cortical neurons

To evaluate the *in vitro* cytotoxicity of the alkaloidal fractions, the percentage of LDH released into the medium was quantified between DIV 7 and DIV 8 (Fig. 2A), and the concentrations selected for the cytotoxicity assay were chosen with respect to a previous reports [17]. The results indicate that the alkaloidal fractions had minimal toxicity in the whole evaluated range. Considering that the interest in knowing their effectiveness at the lowest concentrations, the alkaloidal fractions were evaluated in the neuroprotection assay at concentrations of 0.75, 1.5, 3.0 and 6.0 μg/mL (Fig. 2B).

3.3. The alkaloidal fractions of Z. carinata protect the neuronal cultures against an excitotoxic stimulus generated by Glu

Aβ-mediated neuronal toxicity, inducing synaptic degradation, NFTs, excitotoxicity and cell death, can interfere directly with memory formation mechanisms [36]. In this context, the posttreatment evaluation of the alkaloidal fractions is the simile to a pharmacological treatment since the toxic stimulus was previously administered. On the other hand, due to the complexity of AD, prophylactic treatment also takes center stage as a therapeutic alternative, so we also evaluated it in pretreatment conditions. The percentage of LDH released into the medium with the toxic stimulus of Glu at 125 μM for 20 min was 13.40%. At pre- and posttreatment, the alkaloidal fractions showed a concentration-dependent response and strong significant differences with respect to Glu. In fact, the most active concentration for both fractions was 0.75 μg/mL, where the bulbs and leaves in pretreatment showed decreases of 80% and 62% in the percentage of LDH, respectively (Fig. 2B). In the posttreatment conditions, both fractions showed a decrease of 35%. Likewise, as the concentration of the fractions increased, the toxicity tended to increase. The decrease in the percentage of LDH released in the medium compared to that in the condition with Glu indicated that the alkaloidal fractions are protecting the neurons against that toxic stimulus, either by preventing or repairing them before and after the toxic stimulus, respectively. Thus, based on these results, the lowest concentration at which the neuroprotective effect was observed was selected for the following experiments, which was 0.75 μg/mL in both the pre- and posttreatment conditions for the two alkaloidal fractions.

3.4. Treatment with the alkaloidal fractions of Z. carinata decreases lipid peroxidation products in neurons

One of the main markers of oxidative damage by the excitotoxic stimulus of Glu is the generation of MDA, a product of lipid peroxidation of neuronal membranes, and the relationship between the toxic stimulus generated by Glu and the consequent activation of intraneuronal oxidative stress has been widely reported [37,14]. Thus, was evaluate the concentration of MDA after treatment with the alkaloidal fractions, both in the pre- and posttreatment conditions (Fig. 2C). Treatment for 20 min with Glu at 125 μM doubled MDA production from baseline, from 162.79 ± 7.42 to 321.112 ± 22.15 ρmol MDA/million neurons. Pretreatment with the alkaloidal fractions did not decrease MDA production; however, a decrease was observed in the posttreatment conditions, where *Z. carinata* B and *Z. carinata* L at 0.75 μg/mL decreased MDA production by 48.14% and 49.35%, respectively. These results suggest that the alkaloidal fractions inhibit lipid peroxidation, which is one of the primary sources of free radical-mediated injury that directly damages neuronal membranes.

3.5. The alkaloidal fractions of Z. carinata decrease the percentage of condensed nuclei in the presence of an excitotoxic stimulus

The percentage of condensed nuclei was quantified, which provides information about the neurons that are in the process of death (Fig. 2D). As expected, neurons stimulated with Glu at 125 μM showed the highest percentage of condensed nuclei (43.54%), and the medium group represents the basal percentage (14.15%). With a similar effect on the production of MDA, both alkaloidal fractions presented significant differences with respect to Glu, mainly in the posttreatment condition. However, although *Z. carinata* L managed to reduce the percentage of condensed nuclei by 50.92% at posttreatment, *Z. carinata* B showed a greater decrease of condensed nuclei with percentages of 34.52% and 67.85% in the pre- and posttreatment conditions, respectively. Although no relevant differences were observed between the fractions regarding their neuroprotective activities (Fig. 2B), the complement with these results suggests that *Z. carinata* B protects neurons to a greater extent than the alkaloidal fraction of the leaves.

3.6. The alkaloidal fractions of Z. carinata maintain the healthy morphological characteristics of the neuronal cultures against an excitotoxic stimulus

Morphologically, the Glu stimulus resulted in approximately 50% neuronal death, consistent with the results of the condensed nuclei (Fig. 2D and E). Glu at 125 μM for 20 min exerts the maximum toxicity on the neurons, which exhibited degeneration of the actin cytoskeleton as a sign of depolymerization and a loss of dendritic structure, in agreement with our previous studies [38]. Nevertheless, treatment with both fractions decreased this behavior, especially at posttreatment. *Z. carinata* B and *Z. carinata* L maintained the healthy characteristics of neurons, such as reducing condensed nuclei, promoting the recovery of the dendritic structure and the qualitatively increasing the neuronal extensions. The alkaloidal fraction of bulbs showed a higher neuroprotective activity than the fraction of leaves. Therefore, based on all the results (Fig. 2) and the potential exhibited in the *in vitro* assays, the alkaloidal fraction of *Z. carinata* B was selected as the candidate for the *in vivo* assays.

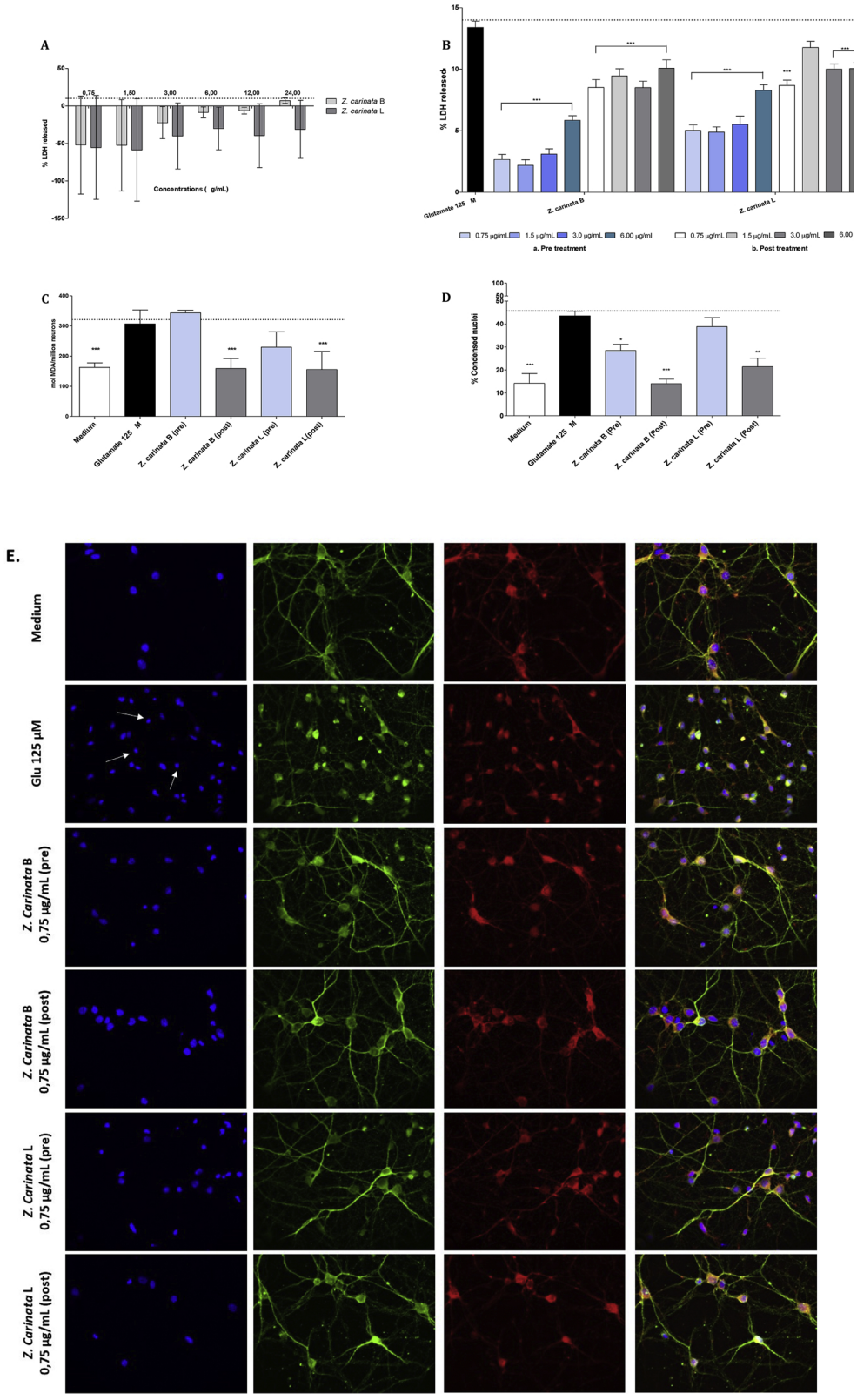

Fig. 2. *In vitro* neuroprotection assay of the alkaloidal fractions of *Z. carinata* against the toxic stimulus Glu. A. Cell viability of primary cerebral cortical neurons exposed to different concentrations of alkaloidal fractions for 24 h as measured by the LDH assay. The toxic level (dashed lines) was considered to be greater than 20% of the LDH released. The results represent the means ± SD of three experiments performed in duplicate; B. Neuroprotective activity of alkaloidal fractions in a neuronal model of Glu excitotoxicity. Pretreatment in blue and posttreatment in gray. The increase in color intensity refers to the increase in the concentration evaluated. Data are expressed as the means ± standard deviation (SD) of at least three independent experiments; *** $p < 0.001$, ** $p < 0.01$, and * $p < 0.05$ vs. excitotoxicity control (Glutamate) in two-way ANOVA with Bonferroni's posttest; C. Quantification of malondialdehyde in neuronal cultures treated with alkaloidal fractions at 0.75 µg/mL; D. Percentage of condensed nuclei of neurons stimulated with 125 µM Glu and treated with alkaloidal fractions at 0.75 µg/mL. Pretreatment in blue and posttreatment in gray (C and D); the results are presented as the mean ± SD (n = 3), and each independent experiment was performed in triplicate; E. Morphological characterization of neurons treated with alkaloidal fractions at 0.75 µg/mL. It shows the nuclei stained with Hoechst (blue), F-actin cytoskeleton stained Phalloidin Alexa 594 dye (red) and dendrites are visualized by staining with MAP2 (green). 40x magnification, scale 20 µM, n = 3. Arrows indicate condensed nuclei and F actin aggregates (For interpretation of the references to colour in this figure legend, the reader is referred to the web version of this article).

3.7. Treatment with Z. carinata B improves the spatial learning and memory task performance of aged 3xTg-AD mice

The MWM is a test to evaluate the behavior, learning and memory dependent on the hippocampus and has been widely used in studies of neurobiology, neuropharmacology and cognitive disorders in rodent models [39]. Therefore, the MWM was used to evaluate the effect of *Z. carinata* B on spatial learning and memory skills. The learning and memory test was started 18 days after the first treatment, and $PS1_{M146V}$ Veh mice, 3xTg-AD Veh mice and 3xTg-AD *Z. carinata* B mice were assessed. At the beginning of the learning test, all the groups showed a similar behavior in the first three trials, since there were no significant

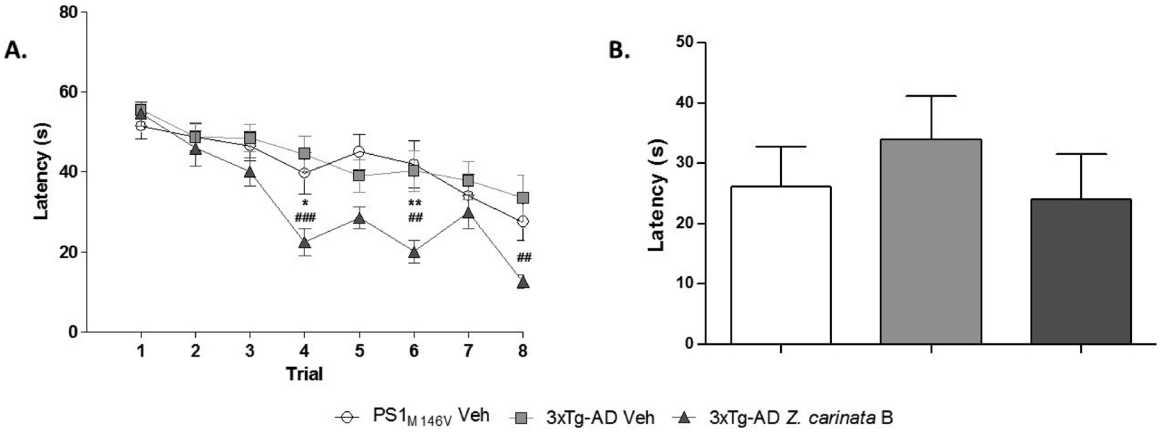

Fig. 3. *Z. carinata* B protects spatial learning and memory function in 3xTg-AD mice. A. Mean latency in reaching the hidden platform on the spatial learning task; B. The latency to reach the platform. The data are expressed as the means ± SEM; n = 7–10; *Compared to the $PS1_{M146V}$ vehicle mice; # compared to the 3xTg-AD vehicle mice; *, # p: < 0.05; **, ## < p: 0.01; ***, ### p: < 0.001.

differences when comparing their arrival latencies to the platform (Fig. 3A). However, from the fourth trial on, the 3xTg-AD mice treated with the alkaloidal fraction exhibited statistically decreased arrival latencies with respect to the control groups. Later, in the retention test, the submerged platform was removed 48 h after the last trial of the learning test to evaluate the hippocampal-dependent memory. The results suggest that, although no significant differences were found between the three groups, the 3xTg-AD Z. *carinata* mice showed a tendency for decrease latency, that is, they exhibited a higher retention performance than the 3xTg-AD vehicle mice (Fig. 3B). Thus, the *Z. carinata* B treatment successfully reversed spatial memory impairment. The visible test did not reveal visual, motor or motivational deficits (data not shown).

3.8. *Z. carinata B treatment in aged 3xTg-AD mice reduces β-amyloidosis*

A large amount of evidence has implicated Aβ as central to the pathogenesis of AD, and it is also widely recognized that age is the most important risk factor of the disease. In fact, in the 3xTg-AD mouse model, the extracellular β-amyloidosis begins to deposit from 6 months of age, and the animals were evaluated at 18 months of age present an Aβ accumulation of more than one year [29]. The fraction of *Z. carinata* B was only evaluated in 3xTg-AD mice, since our interest is to know its effect on the histopathological, as well as cognitive and biochemical, AD markers. As expected, the $PS1_{M146V}$ Veh mice did not exhibit β-amyloidosis in any of the regions studied, and the 3xTg-AD Veh mice displayed strong Aβ immunoreactivity compared with the $PS1_{M146V}$ Veh mice (Fig. 4A). With the alkaloidal fraction treatment, although there were no significant differences between the 3xTg-AD Veh and *Z. carinata* B mice (Fig. 4B and C), there was a trend toward decreased β-amyloid levels by the latter after one month of treatment at a dose of 10 mg/kg i.p. twice per day.

3.9. *Z. carinata B treatment ameliorates tau hyperphosphorylation in aged 3xTg-AD mice*

The neurodegeneration and the development of PHFs and NFTs, which are mainly formed by hyperphosphorylated tau proteins, are postulated as the consequences of the imbalance between the production and the clearance of Aβ [40]. In fact, the intracellular accumulation of tau leads to microtubule disassembly, dendritic collapse and axonal degeneration, which as a result leads to poor communication between neurons and cell death [41]. In the 3xTg-AD model, tau is conformationally altered in the brains of animals from at 18 months old [29]. Thus, this *in vivo* model was used to evaluate the effect of *Z. carinata* B on the decrease of PHFs in the brains of aged 3xTg-AD mice using AT-8 immunoreactivity (Fig. 5A). The 3xTg-AD Veh mice displayed abundant AT-8 immunoreactivity, whereas the 3xTg-AD *Z.*

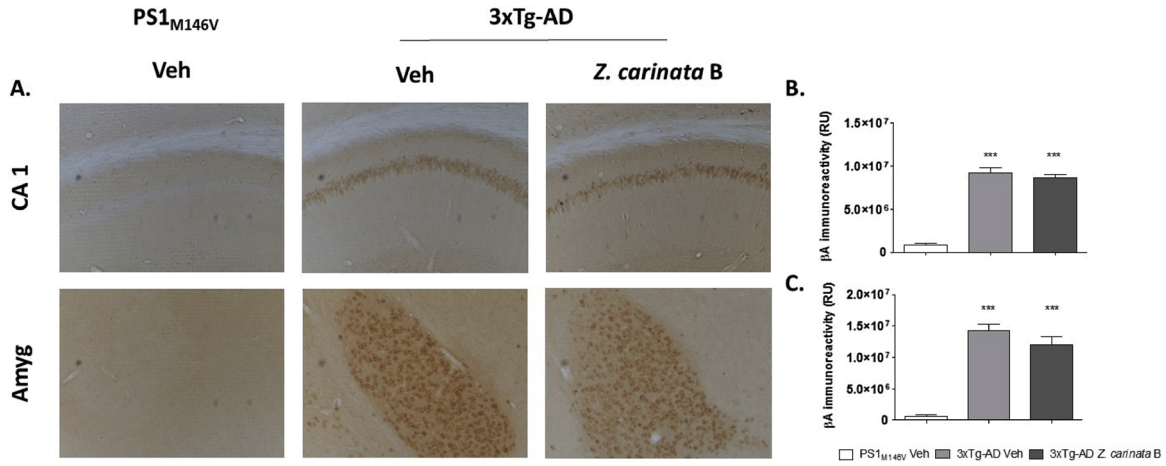

Fig. 4. *Z. carinata* B presents a tendency to decrease β-amyloidosis in the evaluated brain areas. A. Representative images of βA (anti-βA 6E10) immunoreactivity in the CA1 area and the amygdala of $PS1_{M146V}$ vehicle, 3xTg-AD vehicle and 3xTg-AD *Z. carinata* B mice at 19 months of age. Magnification: 10x; scale bar: 50 μm; B and C. The values in the bar graph are expressed in densitometric relative units (RU) of βA immunoreactivity in the CA1 area and in the amygdala, respectively. The data are expressed as the means ± SEM; n = 4–5; *p < 0.05, **p < 0.01, and ***p < 0.001 compared to the $PS1_{M146V}$ vehicle mice.

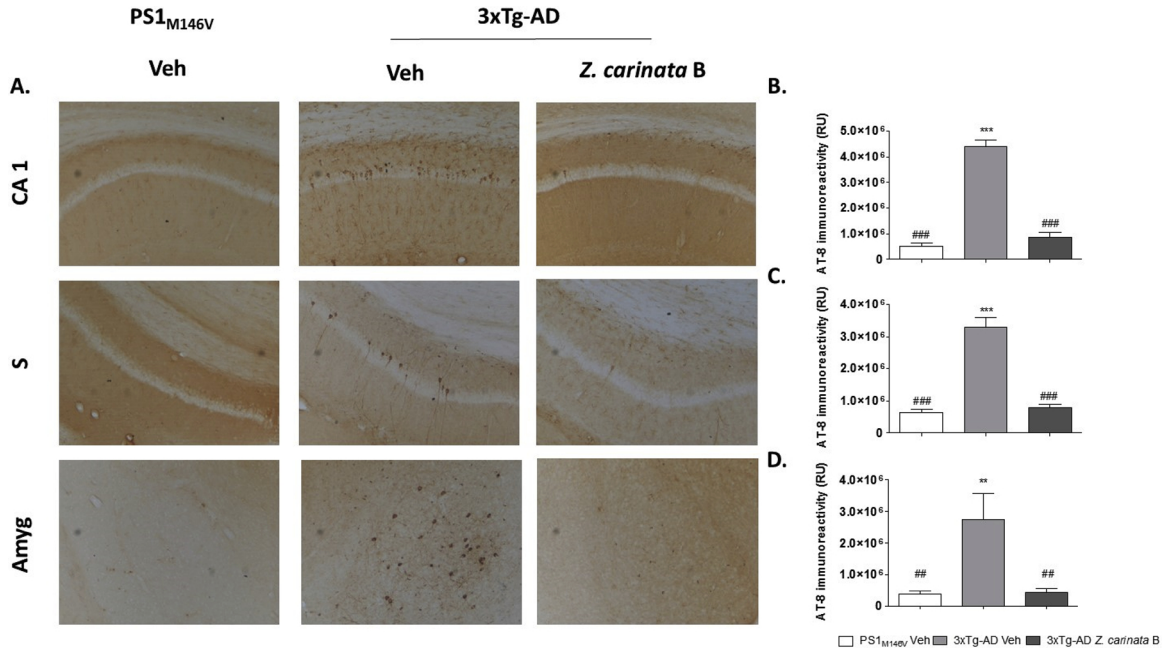

Fig. 5. *Z. carinata* B decreases tauopathy in AD mouse brains. A. Representative images of AT-8 (anti-tau pSer202/Thr205) immunoreactivity in the CA1 area, the subiculum and the amygdala of $PS1_{M146V}$ vehicle, 3xTg-AD vehicle and 3xTg-AD *Z. carinata* B mice. Magnification: 10x; scale bar: 50 μm; B. The values in the bar graph are expressed in densitometric relative units (RU) of AT-8 immunoreactivity in the CA1 area; C. The subiculum and D. The amygdala. *Compared to the $PS1_{M146V}$ vehicle mice; # compared to the 3xTg-AD vehicle mice; *, # p: < 0.05; **, ## < p: 0.01; ***, ### p: < 0.001.

carinata B mice displayed a significant decrease in neurofibrillary tangles in the CA1 area, the subiculum and the amygdala (Fig. 5B–D). The effect directed only toward neurofibrillary tangles suggests that the alkaloidal fraction is a potential selective agent for the treatment of tauopathies.

3.10. Z. carinata B decreases astrogliosis in aged 3xTg-AD mice

In pathological conditions of AD, Aβ is the main factor responsible for inducing and promoting the chronic activation of glial cells, and this response plays a key role in the degenerative cascade of synaptic loss in AD [3]. Reactive astrocytes become part of the inflammatory process when, in addition to microglia, they begin to secrete a series of proinflammatory cytokines and mediators in response to Aβ deposits. This inflammation, called astrogliosis, is a pathological hallmark of AD and is clearly identified by the increased expression of GFAP and the hypertrophy of astrocytes surrounding the Aβ deposits [42]. Thus, astrogliosis is a predominant feature of AD pathology. Therefore, to evaluate whether *Z. carinata* B has an immunomodulatory effect on 3xTg-AD mice, astrogliosis was evaluated *via* GFAP immunoreactivity (Fig. 6A). The data showed a significant increase in GFAP immunoreactivity in the 3xTg-AD and $PS1_{M146V}$ Veh mice; however, there was a significant reduction in the GFAP immunoreactivity in the amygdala of 3xTg-AD *Z. carinata* B mice compared to that in 3xTg-AD Veh mice (Fig. 6B–D). Changes in the CA1 and subiculum area were not observed, and changes in microgliosis with the treatment of *Z. carinata* B were not observed (data not shown).

3.11. Z. carinata B decreases the inflammatory response and promotes survival routes in aged 3xTg-AD mice

Based on the immunohistochemistry results, the effect of the alkaloidal treatment on the expression of proteins involved in neuronal survival and inflammation processes was evaluated in hippocampal lysates. This brain region is known to play an important role in learning, plasticity and memory. It is also one of the areas most affected by β-amyloidosis and tauopathy in the 3xTg-AD model, as shown by Aβ and tau immunolabeling [29,43]. Because the most dramatic histopathological change was the decrease in pair helical filaments (PHFs), the expression of AT-8 (Fig. 7A) and CDK5 (Fig. 7B) was evaluated. Treatment with *Z. carinata* B showed a tendency to decrease the expression of these proteins with respect to the expression in 3xTg-AD Veh mice. However, the expression of pAkt (Fig. 7C), a protein related to neuronal survival, was significantly increased compared to pAkt expression in the 3xTg-AD Veh mice (Fig. 7A). This result suggests that treatment with the alkaloidal fraction has a generalized prosurvival effect throughout the hippocampus, which reinforces the *in vitro* neuroprotection results.

To strengthen the evidence of the anti-inflammatory activity of *Z. carinata* B, the expression of proteins related to this inflammation was also evaluated. The one-month treatment of the alkaloidal fraction resulted in a trend of decreased p38 MAPK and pPLA2/PLA2 expression (Fig. 7D). Nonetheless, COX-2 was significantly upregulated in untreated 3xTg-AD mice compared to the $PS1_{M146V}$ vehicle mice. This inflammatory response was reversed by *Z. carinata* B treatment (Fig. 7E), suggesting an anti-inflammatory effect of the alkaloidal fraction. The results of iNOS expression may suggest that treatment with the alkaloidal fraction for one month at 10 mg/kg twice per day failed to exert an effect on all the proteins related to the main routes of inflammation in the hippocampus.

4. Discussion

Because AD is a chronic disease where Aβ and tau play a fundamental role in the mechanisms of synaptic and neuronal impairment, and glutamate-mediated toxicity is one of the main processes responsible for memory impairment and cell death in AD, two alkaloidal fractions extracted from *Z. carinata* (bulbs and leaves) were evaluated in a Glu excitotoxicity model. This is the first study to provide a complete evaluation of the neuroprotective properties both *in vitro* and *in vivo* of a plant of the family Amaryllidaceae, specifically of *Z. carinata*. The *in vitro* study was performed in pre- and posttreatment conditions, and in both schemes, it is evident that the alkaloidal fractions of bulbs and leaves, at the four concentrations evaluated, present statistical

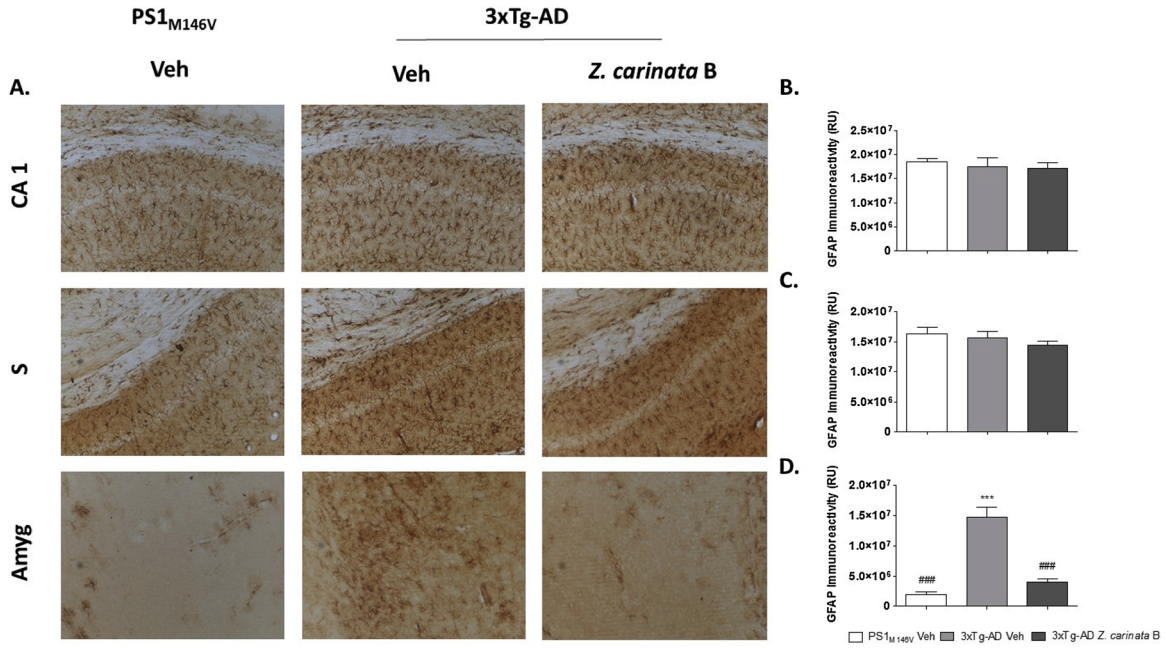

Fig. 6. *Z. carinata* B decreases astrogliosis in the 3xTg-AD mice. A. Representative images of GFAP immunoreactivity in the CA1 area, the subiculum and the amygdala of $PS1_{M146V}$ vehicle, 3xTg-AD vehicle and 3xTg-AD *Z. carinata* B mice. Magnification: 10x; scale bar: 50 μm; B. The values in the bar graph are expressed in densitometric relative units (RU) of GFAP immunoreactivity in the CA1 area; C. The subiculum and D. The amygdala. *Compared to the $PS1_{M146V}$ vehicle mice; # compared to the 3xTg-AD vehicle mice; *, # p: < 0.05; **, ## < p: 0.01; ***, ### p: < 0.001.

differences in the decrease in the percentage of LDH released into the medium compared to the Glu 125 μM cytotoxic condition. The consequent evaluation of the morphological changes of the neurons that were pre- and posttreated with the fractions at the lowest concentration showed that, mainly with the posttreatment, there is a higher percentage of healthy nuclei, a qualitative recovery of the dendritic and a qualitative increase in the neuronal extensions. However, when comparing the two alkaloidal fractions, we concluded that the bulbs are more active than the leaves. This response may be because although both alkaloidal fractions share more than 80% of the alkaloids, the variation in their percentages affects the biological activity. Further, there are four alkaloids that are present only in the alkaloidal fraction of the bulbs. Of these, two were identified as tazettine and lycorine, which represent 5.99% and 1.49%, respectively. While there are no reports of the neuroprotective activity of these alkaloids, previous studies showed that these compounds have antioxidant activity [20], a phenomenon that is strongly linked to the toxic effect in the models used for AD, both *in vitro* and *in vivo*. This difference in chemistry, plus its antioxidant activity, could explain in part the differences in the results of neuroprotective activity and the percentage of condensed nuclei. The observed effects could also be due partly to a blockade of the NMDA receptors [17], however, other receptors could be modulated by

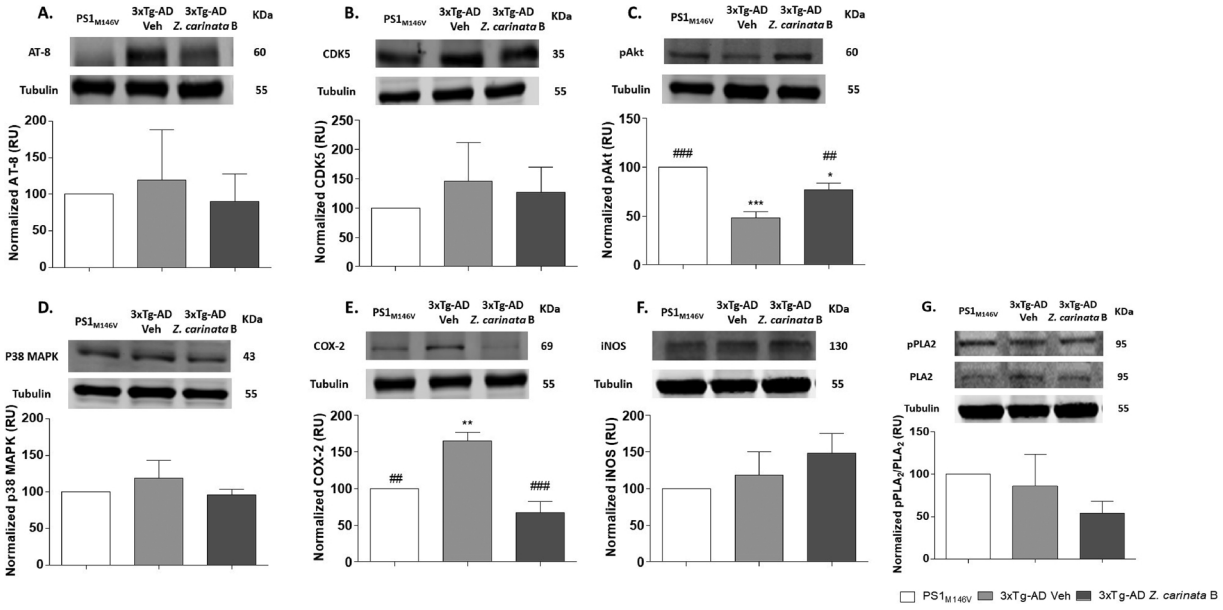

Fig. 7. *Z. carinata* B promotes survival pathways and reduces the proinflammatory response in 3xTg-AD mice. Representative bands and densitometric intensities of A. AT-8; B. CDK5; C. pAKT; D. p38 MAPK; E. COX-2; F. iNOS and G. $pPLA_2/PLA_2$ in hippocampal lysates. *Compared to the $PS1_{M146V}$ vehicle mice; # compared to the 3xTg-AD vehicle mice; *, # p: < 0.05; **, ## < p: 0.01; ***, ### p: < 0.001.

the alkaloids present in the fractions. The ability of galantamine to activate nicotinic receptors [44] suggests that other ways may be involved.

Given that the evidence shows that the therapeutic potential of the fractions occurs mainly when the toxic stimulus has already been generated and that the fraction of the bulbs of *Z. carinata* presented greater neuroprotective activity, we evaluated the potential of *Z. carinata* B in a model of aged 3xTg-AD mice. The results from the MWM corroborate an effect on the cognitive deficits, although there was not a difference between the $PS1_{M146V}$ and 3xTg-AD mice treated with vehicle, as in previous studies [49,50], perhaps due to the advanced age and generation of the colony (F14); nevertheless, the treated 3xTg-AD animals exhibited a statistically decreased latency to find the platform compared with the two control groups of animals. This could be related to the cholinergic hypothesis established for the Alzheimer's disease [45]. In previous studies, the inhibitory activity of *Z. carinata* against the human enzymes AChE and BChE was established [20]. The alkaloidal fraction presented IC_{50} values of 14.91 μg/mL and 27.26 μg/mL for human enzymes AChE and BChE, respectively [20], suggesting that some alkaloids that make up the fraction may exhibit effects upon impaired cholinergic function. Galantamine, an Amaryllidaceae alkaloid approved for the symptomatic treatment of AD, is an inhibitor of the AChE enzyme, and it has been reported that in murine and human models, the concentration of ACh increases in the synaptic cleft of cholinergic neurons after the use of the alkaloid [45]. Therefore, these results suggest that some alkaloids found in the *Z. carinata* B fraction can attenuate the deficits in spatial memory in the 3xTg-AD model.

The behavioral symptoms of AD correlate with the accumulation of plaques and tangles, and they are a direct consequence of the damage and destruction of synapses that mediate memory and cognition [29] was evaluate the clearance of Aβ. This histopathological hallmark of the amyloidogenic hypothesis showed a weak tendency to be reduced by the *Z. carinata* B treatment. However, the production and extracellular aggregation of Aβ in the hippocampus and amygdala of the mice are present beginning at nine months old [29], and the treatment during a month with the alkaloidal fraction at 10 mg/kg after 18 months of aging presented slight modifications. The low dose and the duration of the treatment were possibly not enough to generate a greater effect on Aβ. Inversely, the tauopathy process with this same treatment scheme had a strong statistical decrease on PHF aggregation in the hippocampus, subiculum and amygdala compared to the controls. These results show the first evidence that the administration of the alkaloidal fraction of *Z. carinata* B for one month can reduce the accumulation of PHFs in 3xTg-AD mice. In fact, the cognitive decline is more associated with the accumulation of PHFs than Aβ plaques, hypothesis supported by the correlation of the density of PHF with impairment in AD [40,46]. It is possible that changes in the activity of proteins related to phosphorylation of tau, the main component of PHF, explain the decrease of this histopathological marker with the treatment of *Z. carinata* B. Recently, alkaloids type galanthamine, crinine and tazettine (identified cores in *Z. carinata* B) have reported some inhibitory activity of glycogen synthase kinase-3β (GSK-3β), one of the proteins responsible for the hyperphosphorylation of tau protein [47]. On the other hand, an increase in the GFAP reactivity was observed in the aged $PS1_{M146V}$ Veh mice. Aβ plaques are surrounded by reactive astrocytes, where the role of activated glial cells is considered as an endogenous defensive mechanism against plaque deposition, and their constant activation leads to inflammatory processes associated with AD progression [3]. The background during the pathogenesis of AD is an aging process, where there is an inflammatory phenotype comparable with the 3xTg-AD mouse model. This is how senescence, a process characterized by the functional alteration of the cell, is accompanied by the production of molecules that affect neighboring cells, creating a proinflammatory environment [3]. Interestingly, *Z. carinata* B alkaloid treatment decreased astrogliosis, mainly in the amygdala. This result suggests that the treatment might be intervening in the inflammatory processes triggered by the production of Aβ. However, as in the case of β-amyloidosis, the concentration of the alkaloids responsible for these activities may not have been high enough within the fraction (10 mg/kg), preventing evidence of a greater effect.

Although with this treatment scheme, we have not shown a decrease in the labeling of reactive astrocytes in the hippocampus, a structure that is particularly vulnerable to the aging process and to deficits in learning and spatial memory, and the observations of PHFs led to the evaluation of the expression of proteins related to inflammation, survival and tauopathy. Treatment for one month with *Z. carinata* B showed a tendency to reduce the inflammatory marker p38 MAPK. However, the most interesting change was in COX-2, since there was a statistically significant decrease in its expression throughout the hippocampus. Simultaneously, treatment with the alkaloidal fraction down regulated pPLA2/PLA2, phospholipid-metabolizing enzymes, suggesting that there is a tendency to decrease the altered metabolism of phospholipids [48]. This result corroborates the *in vitro* effect of *Z. carinata* B on the decrease in MDA, a marker of lipid peroxidation, during posttreatment. Additionally, the results of pAKT, a protein related to survival processes, indicated that there was a significant increase in pAKT expression caused in the treated mice with respect to the untreated 3xTg-AD mice. These results together indicate that treatment with *Z. carinata* B can intervene in the processes related to neuronal survival and inflammation throughout the hippocampus, whose structure and functional integrity are crucial for normal learning and may explain the functional recovery in the alkaloid-treated AD mice.

Therefore, the *in vitro* and *in vivo* protective activities induced by *Z. carinata* B indicate that the alkaloids that make up this fraction have the potential for palliative treatment and modulation of AD, since their alkaloids affected different targets and generated a global recovery of the disease. Nevertheless, the proposal of the pharmacological use of a fraction with several alkaloids can be very difficult, being that very complex pharmacokinetics could result, requiring extensive preclinical studies to estimate the benefit, side-effects and potential drug interactions. Although the compliance issue can be resolved by combining several alkaloids into a single pill (polypharmacological strategy), to do this, it is necessary to determine the alkaloids that are responsible for the various neuroprotective effects. This last issue is already being undertaken in our laboratory.

5. Conclusion

In summary, the results of *in vitro* neuroprotection, which are based on excitotoxicity, are a platform to evaluate and consequently postulate an alkaloidal fraction as a neuroprotective agent in an *in vivo* model for AD. The correlation between the results of the treatment with *Z. carinata* B in the enzymatic inhibition tests with the MWM test, the excitotoxicity with the aggregation of PHFs, the inflammatory activity and the lipid peroxidation indicate that the chemistry of this fraction has a great potential as a polypharmacological agent for the treatment of AD.

Conflicts of interest

The authors declare no conflicts of interest.

Acknowledgments

We would to thank to Tania Marquez Durango for her veterinarian support at mice colony maintenance in UdeA´s SPF vivarium. This investigation received financial support from COLCIENCIAS (agreement # 452-2013). The authors express their gratitude to the Iberian-American Programme for Cooperation and Development (CYTED) (Ref. 416RT0511) – BIFRENES Thematic Network.

References

[1] A. Dey, et al., Natural products against Alzheimer's disease: Pharmaco-therapeutics and biotechnological interventions, Biotechnol. Adv. 35 (2) (2017) 178–216, https://doi.org/10.1016/j.biotechadv.2016.12.005.

[2] Dementia statistics 2018 | Alzheimer's Disease International (no date) Available at: https://www.alz.co.uk/research/statistics (Accessed 14 November 2017).

[3] L.M. Osborn, et al., Astrogliosis: An integral player in the pathogenesis of Alzheimer's disease, Prog. Neurobiol. 144 (2016) 121–141, https://doi.org/10.1016/j.pneurobio.2016.01.001.

[4] G.S. Bloom, Amyloid-β and tau, JAMA Neurol. 71 (4) (2014) 505, https://doi.org/10.1001/jamaneurol.2013.5847.

[5] Z. Esposito, et al., Amyloid β, glutamate, excitotoxicity in Alzheimer's disease: are we on the right track? CNS Neurosci. Ther. 19 (8) (2013) 549–555, https://doi.org/10.1111/cns.12095.

[6] Y. Zhang, et al., Dysfunction of NMDA receptors in Alzheimer's disease, Neurol. Sci. 37 (7) (2016) 1039–1047, https://doi.org/10.1007/s10072-016-2546-5.

[7] R. Medeiros, F.M. LaFerla, Astrocytes: conductors of the Alzheimer disease neuroinflammatory symphony, Exp. Neurol. 239 (2013) 133–138, https://doi.org/10.1016/j.expneurol.2012.10.007.

[8] R. Briggs, S.P. Kennelly, D. O'Neill, Drug treatments in Alzheimers disease, Clin. Med. 16 (3) (2016) 247–253, https://doi.org/10.7861/clinmedicine.16-3-247.

[9] M. Rosini, et al., Multitarget strategies in Alzheimer's disease: benefits and challenges on the road to therapeutics, Future Med. Chem. 8 (6) (2016) 697–711, https://doi.org/10.4155/fmc-2016-0003.

[10] P. Busquet, et al., Synergistic effects of galantamine and memantine in attenuating scopolamine-induced amnesia in mice, J. Pharmacol. Sci. 120 (4) (2012) 305–309.

[11] P.G. Yanev, D.S. Dimitrova, D.P. Getova-Spassova, Effects of rivastigmine and memantine alone and in combination on learning and memory in rats with scopolamine-induced amnesia, Open Med. 10 (1) (2015) 338–345, https://doi.org/10.1515/med-2015-0050.

[12] R. Tundis, et al., Natural compounds and their derivatives as multifunctional agents for the treatment of alzheimer disease, Discovery and Development of Neuroprotective Agents from Natural Products, (2018), pp. 63–102, https://doi.org/10.1016/B978-0-12-809593-5.00003-3.

[13] Y. Ding, et al., Phytochemical and biological investigations of Amaryllidaceae alkaloids: a review, J. Asian Nat. Prod. Res. 19 (1) (2017) 53–100, https://doi.org/10.1080/10286020.2016.1198332.

[14] J. Li, et al., Oxidative stress and neurodegenerative disorders, Int. J. Mol. Sci. 14 (12) (2013) 24438–24475, https://doi.org/10.3390/ijms141224438.

[15] X. Li, et al., Neuroprotective compounds from the bulbs of *Lycoris radiata*, Fitoterapia 88 (2013) 82–90.

[16] N. Cortes, R. Alvarez, et al., Alkaloid metabolite profiles by GC/MS and acetylcholinesterase inhibitory activities with binding-mode predictions of five Amaryllidaceae plants, J. Pharm. Biomed. Anal. 102 (2015) 222–228, https://doi.org/10.1016/j.jpba.2014.09.022.

[17] N. Cortes, R.A. Posada-Duque, et al., Neuroprotective activity and acetylcholinesterase inhibition of five Amaryllidaceae species: a comparative study, Life Sci. 122 (2015) 42–50, https://doi.org/10.1016/j.lfs.2014.12.011.

[18] M.M. Svedberg, I. Bednar, A. Nordberg, Effect of subchronic galantamine treatment on neuronal nicotinic and muscarinic receptor subtypes in transgenic mice overexpressing human acetylcholinesterase, Neuropharmacology 47 (4) (2004) 558–571.

[19] J.K. Kim, S.U. Park, Pharmacological aspects of galantamine for the treatment of Alzheimer's disease, EXCLI J. 16 (2017) 35–39, https://doi.org/10.17179/excli2016-820.

[20] N. Cortes, et al., Alkaloids of Amaryllidaceae as inhibitors of cholinesterases (AChEs and BChEs): An integrated bioguided study, Phytochem. Anal. 29 (2) (2018) 217–227, https://doi.org/10.1002/pca.2736.

[21] C.G. Guerrieri, et al., Alkaloids from Crinum erubescens Aiton, Arab. J. Chem. 9 (5) (2016) 688–693, https://doi.org/10.1016/j.arabjc.2015.07.009.

[22] S. Berkov, J. Bastida, B. Sidjimova, et al., Phytochemical differentiation of Galanthus nivalis and Galanthus elwesii (Amaryllidaceae): a case study, Biochem. Syst. Ecol. 36 (8) (2008) 638–645, https://doi.org/10.1016/j.bse.2008.04.002.

[23] G. Banker, K. Goslin, Culturing Nerve Cells, second ed., (1998) Cambridge, Massachusetts.

[24] A. Lopez-Tobón, E. Cepeda-Prado, G.P. Cardona-Gómez, Decrease of Tau hyperphosphorylation by 17β estradiol requires sphingosine kinase in a glutamate toxicity model, Neurochem. Res. 34 (12) (2009) 2206–2214, https://doi.org/10.1007/s11064-009-0017-6.

[25] J.C. Gallego-Gómez, et al., Differences in virus-induced cell morphology and in virus maturation between MVA and other strains (WR, Ankara, and NYCBH) of vaccinia virus in infected human cells, J. Virol. 77 (19) (2003) 10606–10622.

[26] J. Gutiérrez, et al., Rac1 activity changes are associated with neuronal pathology and spatial memory long-term recovery after global cerebral ischemia, Neurochem. Int. 57 (7) (2010) 762–773, https://doi.org/10.1016/j.neuint.2010.08.014.

[27] R.A. Posada-Duque, et al., Atorvastatin requires geranylgeranyl transferase-I and Rac1 activation to exert neuronal protection and induce plasticity, Neurochem. Int. 62 (4) (2013) 433–445, https://doi.org/10.1016/j.neuint.2013.01.026.

[28] E. Osorio, J. Londoño, J. Bastida, Low-Density Lipoprotein (LDL)-Antioxidant Biflavonoids from *Garcinia madruno*, Molecules 18 (5) (2013) 6092–6100, https://doi.org/10.3390/molecules18056092.

[29] S. Oddo, et al., Triple-transgenic model of Alzheimer's disease with plaques and tangles: intracellular Abeta and synaptic dysfunction, Neuron 39 (3) (2003) 409–421.

[30] S. Jahn, et al., Metabolic studies of the Amaryllidaceous alkaloids galantamine and lycorine based on electrochemical simulation in addition to in vivo and in vitro models, Anal. Chim. Acta 756 (2012) 60–72, https://doi.org/10.1016/j.aca.2012.10.042.

[31] S. Aronson, et al., Optimal dosing of galantamine in patients with mild or moderate Alzheimer's disease: post Hoc analysis of a randomized, double-blind, placebo-controlled trial, Drugs Aging 26 (3) (2009) 231–239.

[32] R.G. Morris, et al., Place navigation impaired in rats with hippocampal lesions, Nature 297 (5868) (1982) 681–683.

[33] K.B.J. Franklin, G. Paxinos, Paxinos and Franklin's the Mouse Brain in Stereotaxic Coordinates, fourth ed., Academic Press, 2012.

[34] P. Cardona-Gomez, et al., Estradiol inhibits GSK3 and regulates interaction of estrogen receptors, GSK3, and beta-catenin in the hippocampus, Mol. Cell. Neurosci. 25 (3) (2004) 363–373, https://doi.org/10.1016/j.mcn.2003.10.008.

[35] S. Berkov, J. Bastida, F. Viladomat, et al., Analysis of galanthamine-type alkaloids by capillary gas chromatography–mass spectrometry in plants, Phytochem. Anal. 19 (4) (2008) 285–293, https://doi.org/10.1002/pca.1028.

[36] V. Campos-Pea, M. Antonio, Alzheimer disease: the role of aβ in the glutamatergic system, Neurochemistry, InTech, 2014, https://doi.org/10.5772/57367.

[37] E. Niedzielska, et al., Oxidative stress in neurodegenerative diseases, Mol. Neurobiol. 53 (6) (2016) 4094–4125, https://doi.org/10.1007/s12035-015-9337-5.

[38] R.A. Posada-Duque, V. Palacio-Castañeda, G.P. Cardona-Gómez, CDK5 knockdown in astrocytes provide neuroprotection as a trophic source via Rac1, Mol. Cell. Neurosci. 68 (2015) 151–166, https://doi.org/10.1016/j.mcn.2015.07.001.

[39] R. Schoenfeld, et al., Variants of the Morris water maze task to comparatively assess human and rodent place navigation, Neurobiol. Learn. Mem. 139 (2017) 117–127, https://doi.org/10.1016/j.nlm.2016.12.022.

[40] K.R. Brunden, J.Q. Trojanowski, V.M.-Y. Lee, Advances in tau-focused drug discovery for Alzheimer's disease and related tauopathies, Nat. Rev. Drug Discov. 8 (10) (2009) 783–793.

[41] J.T. Pedersen, E.M. Sigurdsson, Tau immunotherapy for Alzheimer's disease, Trends Mol. Med. 21 (6) (2015) 394–402, https://doi.org/10.1016/j.molmed.2015.03.003.

[42] A. Verkhratsky, et al., Astroglia dynamics in ageing and Alzheimer's disease, Curr. Opin. Pharmacol. 26 (2016) 74–79, https://doi.org/10.1016/j.coph.2015.09.011.

[43] Y. Mu, F.H. Gage, Adult hippocampal neurogenesis and its role in Alzheimer's disease, Mol. Neurodegener. 6 (1) (2011) 85, https://doi.org/10.1186/1750-1326-6-85.

[44] J. Coyle, P. Kershaw, Galantamine, a cholinesterase inhibitor that allosterically modulates nicotinic receptors: effects on the course of Alzheimer's disease, Biol. Psychiatry 49 (3) (2001) 289–299.

[45] J.E. Sweeney, P.S. Puttfarcken, J.T. Coyle, Galanthamine, an acetylcholinesterase inhibitor: a time course of the effects on performance and neurochemical parameters in mice, Pharmacol. Biochem. Behav. 34 (1) (1989) 129–137.

[46] D.T. Jones, et al., Tau, amyloid, and cascading network failure across the Alzheimer's disease spectrum, Cortex 97 (2017) 143–159, https://doi.org/10.1016/J.CORTEX.2017.09.018.

[47] D. Hulcová, et al., Amaryllidaceae alkaloids as potential glycogen synthase kinase-3β inhibitors, Molecules 23 (4) (2018) 719, https://doi.org/10.3390/molecules23040719.

[48] G. Di Paolo, T.-W. Kim, Linking lipids to Alzheimer's disease: cholesterol and beyond, Nat. Rev. Neurosci. 12 (5) (2011) 284–296, https://doi.org/10.1038/nrn3012.

[49] A.M. Sabogal-Guáqueta, et al., The flavonoid quercetin ameliorates Alzheimer's disease pathology and protects cognitive and emotional function in aged triple transgenic Alzheimer's disease model mice, Neuropharmacology 93 (2015) 134–145, https://doi.org/10.1016/j.neuropharm.2015.01.027.

[50] A.M. Sabogal-Guáqueta, E. Osorio, G.P. Cardona-Gómez, Linalool reverses neuropathological and behavioral impairments in old triple transgenic Alzheimerás mice, Neuropharmacology 102 (2016) 111–120, https://doi.org/10.1016/j.neuropharm.2015.11.002.